

Shared Causal Paths underlying Alzheimer's dementia and Type 2 Diabetes

Zixin Hu¹, Rong Jiao², Jiucun Wang^{1,3}, Panpan Wang¹, Yun Zhu⁴, Jinying Zhao⁴, Phil De Jager⁵, David A Bennett⁶, Li Jin^{1,3} and Momiao Xiong^{2*}

Background: Although Alzheimer's disease (AD) is a central nervous system disease and type 2 diabetes mellitus (T2DM) is a metabolic disorder, an increasing number of genetic epidemiological studies show clear link between AD and T2DM. The current approach to uncovering the shared pathways between AD and T2DM involves association analysis; however, such analyses lack power to discover the mechanisms of the diseases.

Methods: We develop novel statistical methods to shift the current paradigm of genetic analysis from association analysis to deep causal inference for uncovering the shared mechanisms between AD and T2DM, and develop pipelines to infer multilevel omics causal networks which lead to shifting the current paradigm of genetic analysis from genetic analysis alone to integrated causal genomic, epigenomic, transcriptional and phenotypic data analysis. To discover common causal paths from genetic variants to AD and T2DM, we also develop algorithms that can automatically search the causal paths from genetic variants to diseases and

Results: The proposed methods and algorithms are applied to ROSMAP dataset with 432 individuals who simultaneously had genotype, RNA-seq, DNA methylation and some phenotypes. We construct multi-omics causal networks and identify 13 shared causal genes, 16 shared causal pathways between AD and T2DM, and 754 gene expression and 101 gene

methylation nodes that were connected to both AD and T2DM in multi-omics causal networks.

Conclusions: The results of application of the proposed pipelines for identifying causal paths to real data analysis of AD and T2DM provided strong evidence to support the link between AD and T2DM and unraveled causal mechanism to explain this link.

Keywords: Causal inference, additive noise models, structural equations, shared genes and pathways, Alzheimer's Disease and type 2 diabetes.

¹State Key Laboratory of Genetic Engineering and Innovation Center of Genetics and Development, School of Life Sciences, Fudan University, Shanghai, China.

²Department of Biostatistics and Data Science, School of Public Health, University of Texas Health Science Center at Houston, Houston, Texas, USA.

³Human Phenome Institute, Fudan University, Shanghai, China.

⁴Department of Epidemiology, University of Florida, Florida, USA

⁵ Center for Translational & Computational Neuroimmunology, Department of Neurology, Columbia University Medical Center, New York, 10033, USA

⁶ Rush Alzheimer's Disease Center, Rush University Medical Center, Chicago, IL 60612, USA

Background

Although Alzheimer's dementia is a central nervous system disease and type 2 diabetes mellitus (T2DM) is a metabolic disorder, an increasing number of epidemiological and genetic epidemiological studies show clear link between Alzheimer's dementia and T2DM. Alzheimer's dementia with great economic, political and social consequences is a progressive, irreversible degenerative disease of the brain and is the most common cause of dementia due to the gradual accumulation of amyloid-beta ($A\beta$) and twisting of tau protein [1, 2], and other common brain pathologies [3]. Alzheimer's dementia is also involved in inflammation and oxidative stress and exhibits memory loss and cognitive dysfunction [4, 5].

Two mechanisms underlying T2DM are insulin resistance and insufficient insulin secretion from pancreatic β -cells [4]. T2DM patients are unable to process insulin signaling correctly that lead to the insulin-resistant. In response to insulin resistance, pancreatic β -cells increase insulin production. However, when pancreatic β -cells gradually lose function; insulin production cannot be increased to maintain normal glucose levels. The brain is a target organ for insulin [6]. Insulin signaling plays an important role in the organization and function of the brain and impaired insulin signaling induces an overactivation of GSK-3 kinase, increases tau phosphorylation, alters tau modification and causes neurofibrillary degeneration [7]. T2DM also suffer from mild to severe nervous system damage. Persistent blood glucose increases may impair blood flow to the brain [8].

Prior work in ROSMP found an association of T2DM with incident Alzheimer's dementia and rate of cognitive decline [9]. However, we did not find an association with Alzheimer's disease (AD) pathology [10]. Rather, we found an association with cerebral infarcts. Other evidence from ROSMP continue to point to potential common mechanisms. For example, we found that

brain insulin signaling was associated with AD pathology [11]. We also found interactions between *GSKβ* polymorphisms associated with β-amyloid deposition [12].

The current approaches to identifying several shared pathophysiology processes between Alzheimer's dementia and T2DM have several limitations. Firstly, the most previous works have focused on identifying biological pathways underlying AD and T2MD. Few attempts to discover the role of dysregulated SNPs, gene expressions and methylations have been carried out. Secondly, the conventional evidences for linking AD and T2MD purely depend on the statistical association [13]. Numerous association studies strongly demonstrate that association analysis lacks power to discover the mechanisms of the diseases for the two major reasons. The first reason is that association and causation are different concepts. Association is to characterize the trend pattern between two variables, while causation between two variables is defined as independence between the distribution of cause and conditional distribution of the effect, given cause. There are three scenarios: (1) presence of both association and causation between two variables, (2) presence of association, while absence of causation and (3) presence of causation, while lack of association in causal analysis. If causation loci were searched only from association loci, many causation loci might be missed. The second reason is that the widespread networks that are constructed in integrated omic analysis are undirected graphs. Using undirected graphs, we are unable to infer direct cause-effect relations and hence cannot discover chain of causal mechanism from genetic variation to diseases via gene expressions, epigenetic variation, physiological and phenotype variations. Causal inference coupled with multiple omics, imaging, physiological and phenotypic data is an essential component for the discovery of disease mechanisms.

It is time to develop a new generation of genetic analysis for shifting the current paradigm of genetic analysis from association analysis to deep causal inference and from genetic analysis alone to integrated causal genomic, epigenomic, and phenotypic data analysis for unraveling the mechanistic link between AD and T2DM. To make the shift feasible, we need (1) to develop novel causal inference methods for genetic studies of AD and T2DM; (2) to develop unified frameworks for systematic causal analysis of integrated genomic, epigenomic, and clinical phenotype data and to infer multilevel omics causal networks for the discovery of common paths from genetic variants to AD and T2DM via methylations, gene expressions and multiple phenotypes. The real data set ROSMAP [14, 15] will be used to validate the multilevel omics causal networks as a general framework for identifying shared causal paths between AD and T2DM and demonstrates that the proposed methods are capable of identifying the shared pathologic paths between AD and T2DM. A program for implementing the algorithm for construction of multilevel causal networks can be downloaded from our website <https://sph.uth.edu/research/centers/hgc/xiong/software.htm>.

Methods

ROSMAP Data

The data came from two longitudinal cohort studies of older persons, ROS that started in 1994 and enrolled Catholic nuns, priests, and brothers from more than 40 communities across United States, and MAP that started in 1997 and enrolled participants with diverse backgrounds and socioeconomic status from continuous care retirement communities throughout northeastern Illinois, as well as from individual homes across the Chicago metropolitan area [34]. These two studies are managed by the same team of investigators. Structured, quantitative neuropathological examinations are performed at a single site. Therefore, the data can be combined in the analysis. Multi-layered omics datasets are generated from biospecimens donated by ROS and MAP participants, including genotypes, DNA methylation profiles and RNA-seq. The genotype data were generated by Affymetrix or the Illumina OmniQuad express gene chips and were imputed using the 1000 Genomes Project data as reference. DNA methylation profiles were measured using the Illumina Infinium HumanMethylation450 beadset. RNA-seq data were generated using the Illumina HiSeq with 101bp paired-end reads. Multiple phenotypes including clinical diagnosis, cognitive function, measures of lifestyle, behavior, and activity, chronic medical conditions and risk factors were measured. A total of 432 individuals who simultaneously had genotype, RNA-seq, DNA methylation and some phenotypes were included in analysis. In the analysis, we considered 19 phenotypes and environments, two diseases (AD, T2DM), 299 pathways with RNA-Seq in KEGG pathway database, 20,242 methylation genes with 364,661 CpG sites, and 51,060 genotyped genes with 5,711,541 SNPs (4,283,876 common snp, 1,427,665 rare snp).

Genome-wide Causation Studies

Unlike GWAS where we test the association of each variant across the genome with the disease, genome-wide causation studies (GWCS) is to test the causation of each variant across the genome to the disease. The additive noise models (ANMs) with discrete variables will be used for GWCS [27-30]. The procedures that use the ANMs for GWCS are summarized as follows [19].

Procedures for Causal Genetic Analysis Using ANM:

1. Fit the following nonlinear integer regression to the data.

$$Y = f(X) + N_Y.$$

$$\text{Calculate the residuals } \hat{N}_Y = Y - \hat{f}(X).$$

2. Fit the following nonlinear integer regression to the data.

$$X = g(Y) + N_X.$$

$$\text{Calculate the residuals } \hat{N}_X = X - \hat{g}(Y).$$

3. Test for independence.

The contingency table and Fisher's exact test can be used to test independence. Let the statistic for testing the independence between \hat{N}_Y and X as $\Delta_{X \rightarrow Y}$ and the statistic for testing the independence between \hat{N}_X and Y as $\Delta_{Y \rightarrow X}$.

The null hypothesis for testing the causation of the variant is

$$H_0 : \text{no causation between variables } X \text{ and } Y .$$

The statistic for testing the causation between two X and Y is defined as

$$T_C = |\Delta_{X \rightarrow Y} - \Delta_{Y \rightarrow X}|.$$

When T_C is large, the causation between genetic variant X and disease status Y exists. When $T_C \approx 0$, this indicates that no causal decision can be made. Since the distribution of the test statistic T_C is difficult to calculate, P-value for testing the causation of the variant X can be calculated by permutations.

To improve the performance of causation analysis of rare variants, we first calculate the functional principle component score (FPCS) of the rare variants within a gene [30] to summarize information of all rare variants within the gene. Then, the continuous FPCS are discretized. Finally, the ANMs with discrete variables can be used to test causation of discretized FPCS with the disease.

Structural Equations for Construction of Causal Networks

Directed graphical models and structural equations can be used as a tool to model the complex causal structures among variables [30]. A graphical model consists of nodes and edges. The nodes represent variables and edges represent the dependence structures among variables. A directed graphical model is defined as the graph in which all the inter-node connections have a direction visually denoted by an arrowhead. Directed acyclic graphics (DAGs) are defined as directed graphics with no cycles. In other words, we can never start at a node X , travel edges in the directions of the arrows and get back to the node X . A DAG with nodes encodes conditional dependence structure of the variables Y_1, \dots, Y_n . We define the parents of a node as the nodes pointing directly to it. The concept of parents provides an easy way to read off conditional independence from DAGs.

Traditional regressions describe one-way or unidirectional relationships among variables in which the variables on the left sides of the equations are dependent variables and the variables on the right sides of the equations are explanatory variables or independent variables. The

explanatory variables are used to predict the outcomes of the dependent variables. However, in many cases, there are two ways, or simultaneous relationships between the variables. Variables in some equations are response variables, but will be predictors in other equations. The variables in equations may influence each other. It is difficult to distinguish dependent variables and explanatory variables. The structural equation models (SEMs) are a powerful mathematic tool to describe such data generating mechanism and infer causal relationships among the variables.

The SEMs classify variables into two class variables: endogenous and exogenous variables. The jointly dependent variables that are determined in the model are called endogenous variables. The explanatory variables that are determined outside the model or predetermined are called exogenous variables. In the genotype-phenotype networks, the phenotype variables such as BMI, cognitive function, working memory, are endogenous variables, age, sex, race, environments and genotypes are exogenous variables. In the genotype-expression networks, the gene expressions are endogenous variables and genotypes are exogenous variables. In the methylation-expression networks, gene expressions are endogenous variables and methylations are exogenous variables.

We consider M endogenous variables. Assume that n individuals are sampled. We denote the n observations on the M endogenous variables by the matrix $Y = [y_1, y_2, \dots, y_M]$, where $y_i = [y_{1i}, \dots, y_{ni}]^T$ is a vector of collecting n observation of the endogenous variable i .

Exogenous variables are denoted by $X = [x_1, \dots, x_K]$ where $x_i = [x_{1i}, \dots, x_{ni}]^T$. Similarly, random errors are denoted by $E = [e_1, \dots, e_M]$, where we assume $E[e_i] = 0$ and $E[e_i e_i^T] = \sigma_i^2 I_n$ for $i = 1, \dots, M$. The linear structural equations for modeling relationships among variables can be written as:

$$\begin{aligned}
& y_1\gamma_{11} + y_2\gamma_{21} + \dots + y_M\gamma_{M1} + x_1\beta_{11} + x_2\beta_{21} + \dots + x_K\beta_{K1} + e_1 = 0 \\
& \quad \vdots \\
& y_1\gamma_{1M} + y_2\gamma_{2M} + \dots + y_M\gamma_{MM} + x_1\beta_{1M} + x_2\beta_{2M} + \dots + x_K\beta_{KM} + e_M = 0
\end{aligned} \tag{1}$$

where the γ 's and β 's are the structural parameters of the system that are unknown. Variables in the SEMs can be classified into two basic types of variables: observed variables that can be measured and the residual error variables that cannot be measured and represent all other unmodeled causes of the variables. Most observed variables are random. Some observed variables may be nonrandom or control variables (e. g. genotypes, drug dosages) whose values remain the same in repeated random sampling or might be manipulated by the experimenter. The observed variables will be further classified into exogenous variables, which lie outside the model, and endogenous variables, whose values are determined through joint interaction with other variables within the system. All nonrandom variables can be viewed as exogenous variables. The terms exogenous and endogenous are model specific. It may be that an exogenous variable in one model is endogenous in another.

Traditionally, we often select one endogenous variable to appear on the left-hand side of the equation. Specifically, the i -th equation is

$$y_i = y_1\gamma_{1i} + \dots + y_{i-1}\gamma_{i-1i} + y_{i+1}\gamma_{i+1i} + \dots + y_M\gamma_{Mi} + x_1\beta_{1i} + \dots + x_K\beta_{Ki} + e_i, \tag{2}$$

where γ_{ji} is a path coefficient that measures the strength of the causal relationship from y_j to y_i ,

β_{ki} is a path coefficient from the exogenous variable to the endogenous variable which measure the causal effect of the exogenous variable x_k on the endogenous variable y_i . The coefficients

$\gamma_{ji} = 0$ and $\beta_{ki} = 0$ imply the zero direct influence of Y_j and x_k on Y_i , respectively and are

usually omitted from the equation. Therefore, equation (2) is reduced to

$$\begin{aligned}
y_i &= Y_{-i}\gamma_i + X_i\beta_i + e_i \\
&= W_i\Delta_i + e_i
\end{aligned} \tag{3}$$

where Y_{-i} is a vector of the endogenous variables after removing variable y_i , γ_i is a vector of the path coefficients associated with Y_{-i} , and

$$W_i = [Y_{-i} \quad X_i], \Delta_i = \begin{bmatrix} \gamma_i \\ \beta_i \end{bmatrix}.$$

Multiplying by the matrix X^T on both sides of equation (3), we obtained

$$X^T y_i = X^T W_i \Delta_i + X^T e_i. \quad (4)$$

Estimation of the parameters in the structural equations is rather complex. It involves many different estimation methods with varying statistical properties. We used two stage least squares (2SLS) method to estimate the parameters. In general, the causal networks are sparse. Using weighted least square and l_1 -norm penalization of equation (4), we can form the following optimization problem to estimate the structure of causal network:

$$\min_{\Delta_i} f(\Delta_i) + \lambda \|\Delta_i\|_1 \quad (5)$$

where $f(\Delta_i) = (X^T y_i - X^T W_i \Delta_i)^T (X^T X)^{-1} (X^T y_i - X^T W_i \Delta_i)$.

The alternating direction method of multipliers (ADMM) and proximal methods can be used to estimate the parameters and structure of causal network [30, 67, 68].

Functional Structural Equation Models for Construction of Gene-based Causal Networks

The SEMs carry out variant by variant analysis. However, the power of the traditional variant-by-variant analytical tools for construction of causal networks with rare variants as exogenous variables will be limited. Large simulations have shown that combining information across multiple variants in a genomic region of analysis will greatly enhance the power to infer causal networks with rare variants as exogenous variables. To utilize multi-locus genetic information, we propose to use a genomic region or a gene as a unit in construction of causal networks and develop sparse structural functional equation models (SFEMs) for causal network analysis.

where $\phi_{jl}(t)$, $j = 1, \dots, k$, $l = 1, \dots, L_j$ are the l -th principal component function in the j -th genomic region or gene and η_{njl} are the functional principal component scores of the n -th individual.

Using the functional principal component expansion of $x_{nj}(t)$, we can transform the FSEMs (6) into the traditional multivariate SEMs (1).

Integer Programming for Causal Network learning

Given the dataset, learning causal networks is the task of finding network structures that best fits the data [22]. We used “score and search” methods to learn causal networks via maximizing the score metrics that characterize the causal networks. The “score and search” algorithms consist of two parts: (1) formulate objective function (global score for the whole network) using the score function for each node and (2) search algorithm.

We collected all nodes with directed edges in the causal network into a DAG, denoted as

$G = (V, E)$. The score (objective function) for the DAG G was defined as

$$\text{Score}(G) = \sum_{j \in V} \text{Score}_j(G),$$

where $\text{Score}_j(G)$ was a score for the node j in the network. The $\text{Score}_j(G)$ was calculated as

$f(\Delta_j)$ via solving the optimization problem (5). Therefore, the total score can be decomposed

into a sum of score for all nodes in the DAG. In addition, the $\text{Score}_j(G)$ is entirely determined

by the parent set of the node j in G . A DAG can be encoded by the set $W = \{W_1, \dots, W_p\}$ of

parent variables for all nodes V in the graph G . We use $C(j, W_j)$ to denote a score function for

the pair of node j and its parent set W_j . Therefore, the total score for the DAG G was given by

$$C(D) = \sum_{i \in V} C(v, W_v).$$

The learning task is to find a DAG that optimizes the global score $C(D)$ over all possible DAGs D or parent sets [22]:

$$\min_D \sum_{i \in V, W_i \in D} C(v, W_v).$$

Integer linear programming (ILP) was used as a search algorithm [22]. A DAG learning was formulated as the ILP as follows. We define a variable $x(W_v \rightarrow v)$ to indicate the presence or absence of the parent set W_v in the DAG. In other words, $x(W_v \rightarrow v) = 1$ if and only if it is the parent set for the node v . The parent set W_v can be an empty set. The objective function for the ILP formulation of a DAG learning can be defined as

$$\sum_{v=1}^p \sum_{j=1}^{J_v} C(v, W_{j_v}) x(W_{j_v} \rightarrow v). \quad (7)$$

The goal was to find a candidate parent set W_v for each node v by optimizing the objective function in (7). It is clear that every DAG can be encoded by a zero-one indicator variable. However, any set of zero-one numbers may not encode a DAG. A set of linear constraints must be posted to make the set of indicator variables to represent a DAG. Without constraints all indicator variables for the parent sets will be equal to either zero or one. These solutions will not form a DAG. The constraints need to be imposed to ensure that the solutions encode a DAG.

This constraint that is referred to as convexity constraint, can be expressed as

$$\sum_{i=1}^{I_j} x(W_{i_j} \rightarrow j) = 1, j = 1, \dots, p. \quad (8)$$

The convexity constraints (8) can define a directed graph. However, the generated directed graph may have cycles. To eliminate a cycle, we need to impose the following constraint to ensure that any subset C of the nodes V in a DAG must contain at least one node that has no parent in the subset C

$$\forall C \subseteq \sum_{j \in C} \sum_{W: W \cap C = \emptyset} x(W \rightarrow j) \geq 1, \quad (9)$$

which is referred to as cluster-based constraints. Our goal is to find a candidate parent set W_j for each node j by optimizing objective function (7) subject to the constraints (8) and (9).

The branch and bound method is a popular algorithm ensured to find an optimal solution to the 0-1 ILP problem [22]. Let the LP solution represent “solution of the current linear relaxation”. The basic idea of the branch and bound method is to successively divide the ILP problem into smaller problems that are easy to solve and reduce the search space. Briefly, the branch and bound algorithm is summarized as follows. Step 1: Let \hat{x} be the LP solution. Step 2: if there are valid constraints not satisfied by \hat{x} add them and go to Step 1; otherwise if the solution \hat{x} is an integer then stop, the current problem is solved; otherwise branch on a variable with a non-integer part in \hat{x} to generate two new sub-IP problems. We then again use branch and bound algorithms to solve two sub-ILP problems [22].

Multilevel Causal Networks

Multilevel causal omic networks integrated genotype subnetworks, methylation subnetworks, gene expression subnetworks, the intermediate phenotype subnetworks and multiple disease subnetworks into a single connected multilevel genotype-disease networks to reveal the deep causal chain of mechanisms underlying the diseases [30]. ILP was extended from a single causal network estimation to joint multiple causal network estimations to integrate genomic, epigenomic and phenotype data.

For the convenience of discussion, consider M gene expression variables Y_1, \dots, Y_M , Q methylation variables Z_1, \dots, Z_Q , and K genotype variables X_1, \dots, X_K . Let $pa_D(d)$ be the parent set of the node d including gene expression, methylation and genotype variables. Consider three types of SEMs. First, we consider a general SEM model for the gene expression:

$$Y_d = \sum_{i \in pa_D(d)} f_{di}(Y_i) + \sum_{q \in pa_D(d)} f_{dq}(Z_q) + \sum_{j \in pa_D(d)} f_{dj}(X_j) + \varepsilon_d, \quad d = 1, \dots, M, \quad (10)$$

and

$$Z_q = \sum_{l \in pa_Q(q)} f_{ql}(Z_l) + \sum_{m \in pa_Q(q)} f_{qm}(X_m) + \varepsilon_q, \quad q = 1, \dots, Q, \quad (11)$$

where f_d and f_q are linear functions from $R^{|pa_D|} \rightarrow R$ and $R^{|pa_Q|} \rightarrow R$, respectively, and the errors ε_d and ε_q are independent, following distributions P_{ε_d} and P_{ε_q} , respectively. Equation

(10) define a causal network that connects gene expressions, methylations and genotypes.

Equation (11) define a causal network that connects methylations and genotypes.

Integer Programming as a General Framework for Joint Estimation of Multiple Causal Networks

We collected multiple types of data: genotype, gene expression, methylation, and phenotype and disease data. We wanted to estimate multiple causal networks with different types of data.

The scores of the nodes Y_d and Z_q were, respectively, given by

$$C(Y_d, W_{di}) = Y_d^T (I - D_Y^i ((D_Y^i)^T D_Y^i)^{-1} (D_Y^i)^T) Y_d \quad (12)$$

and

$$C(Z_q, W_{ql}) = Z_q^T (I - D_Z^l ((D_Z^l)^T D_Z^l)^{-1} (D_Z^l)^T) Z_q, \quad (13)$$

where matrices D_Y^i and D_Z^l corresponded to the parent sets W_{di} and W_{ql} .

Let V_E be the set of nodes in the gene expression network and V_M be the set of nodes in the methylation network. Let C_E be a subset of nodes in V_E and C_M be a subset of nodes in V_M . A joint expression and methylation causal network can be formulated as the following ILP:

$$\begin{aligned} \text{Min} \quad & \sum_{d=1}^M \sum_{i \in pa_D(d)} C(d, W_{di}) \chi(W_{di} \rightarrow d) + \sum_{q=1}^Q \sum_{l \in pa_Q(q)} C(q, W_{ql}) \chi(W_{ql} \rightarrow q) \\ \text{s.t.} \quad & \sum_{i \in pa_D(d)} \chi(W_{di} \rightarrow d) = 1, \quad d = 1, \dots, M, \\ & \sum_{l \in pa_Q(q)} \chi(W_{ql} \rightarrow q) = 1, \quad q = 1, \dots, Q, \\ & \forall C_E \subseteq V_E : \sum_{d \in C_E} \sum_{W_d: W_d \cap C_E = \emptyset} \chi(W_d \rightarrow d) \geq 1, \\ & \forall C_M \subseteq V_M : \sum_{q \in C_M} \sum_{W_q: W_q \cap C_M = \emptyset} \chi(W_q \rightarrow q) \geq 1. \end{aligned} \quad (14)$$

Using branch and bound and other methods for solving the ILP, we can solve the ILP problem (14) to obtain the best joint causal genotype-methylation-expression and genotype-methylation network fitting the data.

Summary Statistics for Representation of Groups of Gene Expressions

Generalized low rank models were used to segment (cluster) the data. Principal component analysis (PCA) was used to reduce data dimensions. The PCs were used to summarize the gene expression data in pathways and clusters [69].

Results

Shared genetic loci underlying AD and T2DM.

AD and T2DM result from the interplay of DNA sequence variation and nongenetic factors acting through molecular networks [16-18]. Their etiology is complex with multiple steps between genes and phenotypes. Neither traditional GWAS, nor classical multi-omics analysis can identify the causal paths from genetic variants to diseases because not all these analyses can identify directed paths from genetic variants to diseases through environments, methylations, gene expressions, and phenotypes. To overcome these limitations, we develop a novel general framework for identifying all possible causal paths from genetic variants to diseases. The framework consists of three steps. The first step is to perform genome-wide causation studies (GWCS) where we test causation of each SNP across the genome to the disease. The additive noise model (ANM) with discrete variants will be used to test for causation [19] (Methods). We focused on the rare variants in the paper. The second step is to use integer programming (IP) and various modern causal models [20-22] (Methods) for inferring multilevel genome-wide omic causal networks that integrate genotype subnetworks, environmental subnetworks, methylation subnetworks, gene regulatory subnetworks, intermediate phenotype subnetworks and multiple

disease subnetworks into a single connected multilevel genotype-disease network as shown in Figure 1. The third step is to augment graph theoretical approaches with approximations for developing efficient search algorithms that discover all possible paths starting from the genetic variant node directed to the disease node, including classical Depth First Search (DFS) and Breadth First Search (BFS) algorithms [23-26].

There are two ways to identify shared dysfunctional genes (SNPs) between AD and T2DM. One way is to use ANM with discrete variables and functional data analysis to conduct genome-wide causation analysis [27-30] for unravelling the direct connections between gene nodes and disease nodes to identify the shared dysfunctional genes between AD and T2DM.

Another way is to search the paths from the gene nodes to AD and T2DM in multilevel causal omics networks.

Association and causation are different concepts. Association between two variables is often characterized by dependence between two variables. Causation is a connection of phenomena where one variable acts or intervenes on another variables and leads to its changes. Therefore, the key component of causation is the generation and determination of values of one variable by another. The mechanism of causation is related to the transference of matter, motion and information. Causation is universe. It is a part of universe connection. It is well known that nature consists of autonomous and independent causal generating process modules. These modules will not influence each other [29, 31]. In other words, while output of one module may inform or influence input of another module, the events between modules are independent. In the probabilistic language, mechanism is often represented by conditional distribution. Independent mechanism states that “the conditional distribution of each variable given its causes (i.e., its mechanism) does not inform or influence the other conditional distributions” [29]. In GWCS, we

only consider two variables. In this case, independence of cause and mechanism (ICM) indicates that the conditional distribution of the effect given its cause is independent of distribution of cause. Consider the genetic analysis of alleles (A) with a disease allele A a normal allele a and with the disease (D) (disease D and normal d). The joint density function $P(a, d)$ can be decomposed into

$$\begin{aligned} P(A, D) &= P(A)P(D|A) \\ &= P(D)P(A|D). \end{aligned}$$

In the association analysis, we assess whether A is independent of D or not. The relationship between A and D is symmetric. However, in causal analysis, causations $A \rightarrow D$ and $D \rightarrow A$ are different. They are asymmetric. Assessing causation is to consider the effect of intervention. Causation $A \rightarrow D$ indicates that the effect of A is to give rise to disease. However, disease status D will not generate allele A . Suppose that locus A is disease locus and $A \rightarrow D$. If we change the allele a to allele A , then we assume that biological mechanism $P(D|A)$ responsible for giving rise to disease. This would hold true independent of the distribution (frequencies) of allele A . If the locus A is disease locus, we can find that the distributions (frequencies) of allele A in two different populations are different, but the mechanism $P(D|A)$ would apply in two population. The conditional probability $P(D|A)$ can also be viewed as penetrance of the allele. The marginal distribution $P(A)$ and conditional distribution $P(D|A)$ contain no information about each other. Both continuous and discrete ANMs satisfy the ICM and will be used for GWCS., The proposed method for genome-wide causation analysis and inferring multilevel causal genotype-methylation-expression-phenotype-disease network was applied to the ROSMAP dataset [34] with 432 individuals, 19 phenotypes and environments, two diseases (AD, T2DM), 299 pathways with RNA-Seq in KEGG pathway database, 20,242 methylation genes with 364,661

CpG sites, and 51,060 genotyped genes with 5,711,541 SNPs (4,283,876 common snp, 1,427,665 rare snp) (imputed by 1000 Gnome Data). The inferred genotype-expression-methylation-phenotype-disease network consisted of 2,814 nodes and 22,184 edges where the edges were presented in the network if the path coefficients were significantly from zero with P-values < 0.05 .

Table 1. The number of genes connected to AD and T2DM.

		To T2DM			
		Directly Connected	Indirectly Connected	Both Directly and Indirectly Connected	Not Connected
To AD	Directly Connected	5			13
	Indirectly Connected		682	13	
	Both Directly and Indirectly Connected		20	8	
	Not Connected	17			

There were two ways to connect a gene (or SNP) to AD (T2DM). If a gene (or SNP) showed causation to AD (T2DM) by statistical causal test, then the gene (SNP) was directly connected to AD (T2DM) in the causal network. Such gene (SNP) was called AD (T2DM) directly connected gene (SNP). We may observe the connection between a gene (SNP) and AD (T2DM) via multiple edges (paths) in the constructed multilevel causal network. Then, the gene (SNP) that was indirectly connected to AD (T2DM) via paths in the multilevel causal network was called AD (T2DM) indirectly connected gene (SNP). The number of AD and T2DM directly connected or indirectly connected genes was summarized in Table 1. The total number of genes connected to both AD and T2DM including directly connected and indirectly connected was 759. The genes that were both directly and indirectly connected to both AD and T2DM were summarized in Table S1. The genes that were indirectly connected to AD and both directly and indirectly connected to T2DM were listed in Table S2. Similarly, the genes that were both

directly and indirectly connected to AD and indirectly connected to T2DM were summarized in Table S3.

We also tested causation of 299 pathways in the KEGG pathway database to AD and T2DM (Described in detail in the Methods section). The results were summarized as follows. The number of pathways that were directly connected to both AD and T2DM was 16; the number of pathways that were directly connected to AD and indirectly connected to T2DM was 17; the number of pathways that were directly connected to T2DM and indirectly connected to AD was 18, the number of pathways that were indirectly connected to both AD and T2DM was 114; the number of pathways that were directly connected to AD and not connected to T2DM was 6; the number of pathways that were not connected to AD and directly connected to T2DM was 2.

Then, we investigated shared gene expressions via multilevel causal networks. We summarized the results as follows. The number of expression genes that were directly connected to both AD and T2DM was two genes: GRMD1B, RP1-111D6.3, the number of expression genes that were directly connected to AD, but not directly connected to T2DM was 19 (P-value < 10^{-4} , Table S4) and the number of expression genes that were directly connected to T2DM, but not directly connected to AD was 7 (P-value < 10^{-4} , Table S5). The number of expression genes that were indirectly connected to both AD and T2DM was 725.

Similarly, we can study shared methylation via multilevel causal networks. The number of methylated sites/ genes that were directly connected to AD, but not directly connected to T2DM was 17 (Table S6) and the number of methylated sites/genes that were directly connected to T2DM, but not directly connected to AD was 27 (Table S7). The number of methylated sites/genes that were indirectly connected to both AD and T2DM was 117 (Table S8).

The number of phenotypes that were directly connected to both AD and T2DM was six (Age, CHL, HDL ratio, LDL, Semantic memory and working memory).

Shared CREBBP, MAPK and PI3K-AKT pathways between AD and T2DM

Binding of transcription factors to the cyclic Adenosine Monophosphate (cAMP) response element (CRE) regulates the activity of RNA polymerase. cAMP Response Element binding protein (CREB) is a cellular transcription factor that binds the CRE [32]. CREB-binding protein (CREBBP) and CREB together mediate the conversion of short-term memory to long-term memory and alternate the activity of the β -amyloid ($A\beta$) peptide, which in turn regulates hippocampal-dependent synaptic plasticity [33, 34]. Cognitive function such as working memory is involved in insulin signaling dysfunction and blood glucose levels. It was reported that working memory is linked with T2MD [35-37].

To assess whether CREBBP is a common genetic factor of AD and T2DM, and how CREBBP mediates the development of AD and T2DM, we searched the all possible paths from gene CREBBP to AD and T2DM in the inferred multilevel causal network. The results were shown in Figure 2. Figure 2A plotted the path from CREBBP to AD and T2DM via MAPK and PI3K-AKT signaling pathways. The genes in the MAPK and PI3K-AKT signaling pathways, CREBBP, episodic memory, MMSE, AD and T2DM were then used to further infer causal networks using SEMs and IP. The inferred causal network was shown in Figure 2B. From Figure 2B we observed a path from CREBBP to AD and T2DM via gene connections: $CREBBP \rightarrow CBL \rightarrow MAP2K4 \rightarrow MAPK8 \rightarrow MAPK1 \rightarrow PIK3CA$. MAPK and PI3K-AKT pathways play critical roles in memory.

Shared TTC3, FoxO, MAPK, and PI3K-AKT Pathways between AD and T2DM

Next we presented an example to illustrate shared causal paths that started a gene directly connected to AD and indirectly connected to T2DM. The tetratricopeptide repeat domain 3 (TTC3) gene was an AD causing gene (P-value for causation of AD < 0.0001), but not directly connected to T2DM (P-value for causation of T2DM =0.47). TTC3 is associated with differentiation of neurons [38]. It is reported that a rare TTC3 variant is related with AD [39]. The TTC3–RhoA pathway could be a key determinant of the neuronal development, resulting in detrimental effects on the normal differentiation program [40]. Rho regulates the activation of MAPK pathway [41]. The Forkhead box O (FoxO) transcription factors that affect nervous system amyloid (A β) production, are implicated in the regulation of cell apoptosis and survival, and accelerate the progression of degenerative disease. FoxO pathway is involved in the PI3K/Akt and mitogen-activated protein kinase (MAPK) pathways in neuronal apoptosis in the brain.

FoxOs also can offer protection in the nervous system, reduce toxic intracellular protein accumulations and have potential to limit A β toxicity [42, 43, 34]. Akt-FoxO that suppresses TLR4 signaling in Human Leukocytes is implicated in the development of T2DM [44]. There are increasing evidences that PI3K/AKT pathway are implicated in the development of T2DM [45, 46].

Again, we used the DFS algorithm to search the causal paths from multilevel causal networks. The causal paths from TTC3 to AD and T2DM were shown in Figure 3. The paths from MAPK and PI3K-AKT pathway to AD and T2DM were the same as that in Figure 2. The genes in the FoxO, MAPK and PI3K-AKT signaling pathways, TTC3, and episodic memory, MMSE, weight, AD and T2DM were then used to further infer causal networks using SEMs and IP. The structure of the inferred network was shown in Figure 3B. There were a large number of causal paths from

TTC3 to either AD or T2DM. The shared common causal paths were *TTC3* → *NLK* → *CACNA2D1* → *CNCNG3* → *FOXO1* → *CCNE1* → *CYCS* → *MAPK1* → *PIK3CA* and *TTC3* → *NLK* → *PLK2* → *MAPK8* → *MAPK1* → *PIK3CA*.

Shared Morphine Addiction and Neuroactive Ligand Receptor Interaction Pathways

Morphine addiction has neurotoxic effects and damages to the brain regions that function for learning, memory and emotions [47]. High dose of morphine may increase risk to T2DM [48]. It is also reported that neuroactive ligand receptor interaction pathway is associated with both AD and T2DM [49].

Searching the causal paths from gene *HNF4G* to AD and T2DM via the multilevel causal networks using the DFS algorithm, we found that *HNF4G* was indirectly connected to AD and T2DM. In addition to shared MAPK and PI3K-AKT pathways between AD and T2DM which were discussed in the previous sections, we observed shared two new pathways between AD and T2DM: morphine addiction and neuroactive ligand receptor interaction pathways as shown in Figure S1A. The structure of the inferred network that consisted of shared morphine addiction and neuroactive ligand receptor interaction pathways between AD and T2DM was shown in Figure S1B. There were more than 10 shared causal paths. We observed two shared major causal paths: (1) *HNF4G* → *NLK* → *PLK2* → *MAPK8* → *MAPK1* → *PIK3CA* → *AKT1* and (2) *HNF4G* → *NLK* → *GNGT2* → *PLCB2* → *PLCB1* → *ADRB1*.

Shared Fatty Acid Biosynthesis and Primary Bile Acid Biosynthesis Pathways

Brain function such as intelligence, memory, behavior and concentration are all influenced by brain nutrition [50]. Omega-3 fatty acids affect the fluidity of brain cell membranes, neurotransmitter synthesis and signal transmission and are implicated in AD [51, 52]. Bile acids are involved in cell signaling and immune function. It acts as potent inhibitors of apoptosis and

regulates transcriptional and post-transcriptional events that affect mitochondrial function in neurons [53]. A trend of increased bile acids in AD has been observed [54]. Fatty acid utilization induces insulin resistance [55]. Bile acids are signal molecules and play an important role in regulating metabolism and inflammation. The abnormal bile acids are correlated with changes in insulin secretion, which lead to T2DM [56, 57]. The amyloid precursor protein (APP) is a transmembrane protein. The aggregated amyloid- β ($A\beta$) peptides are generated by sequential proteolytic processing of the APP. Accumulation of $A\beta$ and the APP play an important role in regulating lipid homeostasis including fatty acids, which finally affect the development of AD [58].

Our data also provided evidence to show that fatty acid biosynthesis and primary bile acid biosynthesis pathways were shared pathways between AD and T2DM. Search the multilevel causal networks from APP to AD and T2DM using the DFS algorithm, we identified the shared causal paths from APP to both AD and T2DM, shown in Figure 4A. There were two shared causal paths between AD and T2DM: *APP* \rightarrow *neuroactive ligand receptor interaction* and *APP* \rightarrow *fatty acid biosynthesis* \rightarrow *primary bile acid biosynthesis*. Neuroactive ligand receptor interaction pathway was discussed in the previous section.

Next we presented the causal network structure of the shared genes between AD and T2DM in the two shared causal paths in Figure 4B. We observed two major shared paths from APP to AD and T2DM. One path was *APP* \rightarrow *ACSL4* \rightarrow *ACACA* \rightarrow *NUDT9* \rightarrow *CMC1* \rightarrow *PTPLAD1* \rightarrow *CYP781* \rightarrow *CYP46A1* \rightarrow *working memory* (or *CYP781* \rightarrow *AMACA* \rightarrow *working memory*). Another causal path was *APP* \rightarrow *F2RL3* \rightarrow *PIK3R3* (or *F2RL3* \rightarrow *S1PR3* \rightarrow *PIK3R3*).

To further illustrate the validity of the inferred causal paths, we presented Figure S2 that showed the average levels of expression of the genes in Figure 4 for AD, T2DM and normal

individuals. From Figure 4, Figures S2 and S3, we can observed that the genes along the path $APP \rightarrow F2RL3 \rightarrow PIK3R3$ (or $F2RL3 \rightarrow S1PR3 \rightarrow PIK3R3$) of the individuals with AD were over expressed, and the genes along the path $APP \rightarrow ACSL4 \rightarrow ACACA \rightarrow NUDT9 \rightarrow CMC1 \rightarrow PTPLAD1 \rightarrow CYP781 \rightarrow CYP46A1 \rightarrow working\ memory$ (or $CYP781 \rightarrow AMACA \rightarrow working\ memory$) of the individuals with AD were under expressed. Genetic variation in gene *APP* either regulated over expressed genes or regulated under expressed genes. Both of them caused AD. For the individuals with T2DM, the majority of gene expressions along the causal paths from *APP* to T2DM which were regulated by genetic variation in gene *APP* was under expressed.

Shared Methylated Genes *POU3F2*, *KIF4B* and *TNSL3*, and Dopaminergic Synapse and AMPK Pathways

In this section, we illustrate how a shared gene regulates three shared gene methylations, which in turn regulate the shared pathways. Emerging evidences indicate that methylation alternations to DNA of the brain are linked to Alzheimer's disease [62, 63]. DNA methylation also plays an important role in the pathogenesis of T2DM [63, 64]. In order to better understand the etiology of AD and T2DM, we jointly investigated the genetic variants, DNA methylation and gene expression profiles, multiple phenotypes, AD and T2DM using causal inference pipelines. We found that gene *POU3F2* regulated methylations of *POU3F2*, *KIF4B* and *TMSL3*. Alternations in methylation of three genes directly caused the development of AD and T2DM. Furthermore, methylation levels of three genes regulated gene expressions in dopaminergic synapse and AMPK pathways, which in turn caused AD and T2DM via CHL/HDL Ratio (Figure 5A). Recent advance revealed that Alterations of the dopaminergic system contributes to memory and reward dysfunction and the dopaminergic system may well be involved in the occurrence of AD [59,

60]. Recent studies also unravel that the brain damage in AD is linked to an over-activation of AMPK, which leads to the loss of the ability of neurons to grow axons and the modification of the tau proteins resulting in tangles of tau [65]. The AMPK functions as a key energy sensor. AMPK signaling elicits insulin-sensitizing effects and may be implicated in stimulating glucose up taking in skeletal muscles, fatty acid oxidation in adipose (and other) tissues [66]. Our results showed that genetic variation in gene *POU3F2* regulated gene expressions in dopaminergic synapse and AMPK pathways via methylations of *POU3F2*, *KIF4B* and *TMSL3*, which in turn influences CHL/HDL Ration, and finally led to AD and T2DM (Figure 5A).

Again, we presented the causal network structure of the shared genes between AD and T2DM in the two shared dopaminergic synapse and AMPK pathways in Figure 5B. There were multiple shared directed paths from *POU3F2* to AD and T2DM. A major shared directed path:

m: POU3F2 → *m: LOC644649* → *KDM5C* → *PDPK2* → *XPA* → *MK3R2* → *ELK1* →
AD (or → *CHL* → *T2DM*).

Discussion

This paper addresses several issues for uncovering causal paths shared between AD and T2DM.

The first issue is to shift the current paradigm of genetic analysis from association analysis to deep causal inference for uncovering the shared mechanisms between AD and T2DM. The current paradigm for discovering mechanisms of diseases is association analysis. There is increasing recognition that a large proportion of association signals are not causal signals and causal signals may not be association signals. A large number of causal signals cannot be derived from set of association signals. Only searching causal signals from association analysis, a large proportion of causal signals will be missing. Therefore, the ANMs were developed as practical causal inference methods to identify the genetic variants that cause disease.

Second issue is to shift the current paradigm of genetic analysis from genetic analysis alone to integrated causal genomic, epigenomic, transcriptional and phenotypic data analysis for unraveling the mechanisms of AD and T2DM. The widespread existing omics networks that are constructed in integrated multistep analysis of omics are undirected graphs. Using undirected graphs, we are unable to infer direct cause-effect relations among diversified types of variables at multilevel and hence cannot discover chain of causal mechanism from genetic variation to diseases via omics. In this paper, we develop novel statistical methods for multilevel causal omics network construction and provide pipelines for uncovering shared causal paths between AD and T2DM via gene expressions, DNA methylations, environments and multiple phenotypes.

The third issue is to develop algorithms that can automatically search the causal paths from genetic variants to diseases. The size of multilevel causal omics network is large. The number of nodes of such networks can reach ten thousands. The number of causal paths is huge. Manually searching causal paths from large causal networks is infeasible. To meet the challenge of

searching causal paths from large causal networks, we develop computer representation of large causal networks and algorithms for searching the causal paths.

Conclusion

The results of application of the proposed pipelines for identifying causal paths to real data analysis of AD and T2DM provided strong evidence to support the link between AD and T2DM and unraveled causal mechanism to explain this link. We identified the shared causal genes, gene expressions, DNA methylations and pathways between AD and T2DM. Some of them can be supported by literature and some of them are new. We identified an extremely large number of shared causal paths from genetic variants to both AD and T2DM via DNA methylation, gene expressions and phenotypes. This deep knowledge that uncovered the large number of causal mechanisms of AD and T2DM had profound implication in prevention and treatments of AD and T2DM. This explained why the drugs that were based on inhibition or activation of limited number of paths often failed simply because these limited number of paths cannot cover all causal paths to the diseases. Finally, the empirical evidence that the AD and T2DM shared a large number of causal genes, gene expressions, methylations and pathways supported hypothesis that AD can be considered as “type 3 diabetes”.

References

1. Zhuang, Q. S., Zheng, H., Gu, X. D., Shen, L., Ji, H. F. Detecting the genetic link between Alzheimer's disease and obesity using bioinformatics analysis of GWAS data. *Oncotarget*. **8**, 55915-55919 (2017).
2. Song, M. K., Bischoff, D. S., Song, A. M., Uyemura, K., Yamaguchi, D. T. Metabolic relationship between diabetes and Alzheimer's Disease affected by Cyclo(His-Pro) plus zinc treatment. *BBA Clin*. **7**, 41-54 (2016).
3. Lashley T, Schott JM, Weston P, Murray CE, Wellington H, Keshavan A, Foti SC, Foiani M, Toombs J, Rohrer JD, Heslegrave A, Zetterberg H. Molecular biomarkers of Alzheimer's disease: progress and prospects. *Dis Model Mech*. **8**;11(5) (2018).
4. Fischer, R., Maier, O. Interrelation of oxidative stress and inflammation in neurodegenerative diseases: role of TNF, *Oxidative Med. Cell. Longev*. (Feb 2015) 1–18 ID 610813.
5. Li, X., Song, D., Leng, S. X. Link between type 2 diabetes and Alzheimer's disease: from epidemiology to mechanism and treatment. *Clin Interv Aging*. **10**, 549-560. (2015).
6. Baglietto-Vargas, D., Shi, J., Yaeger, D. M., Ager, R., LaFerla, F. M. Diabetes and Alzheimer's disease crosstalk. *Neurosci Biobehav Rev*. **64**, 272-87 (2016).
7. Pugazhenth, S., Qin, L., Reddy, P. H. Common neurodegenerative pathways in obesity, diabetes, and Alzheimer's disease. *Biochim Biophys Acta*. **1863**, 1037-1045 (2017).
8. Akter, K., Lanza, E. A., Martin, S. A., Myronyuk, N., Rua, M., Raffa, R. B. Diabetes mellitus and Alzheimer's disease: shared pathology and treatment? *Br J Clin Pharmacol*. **71**, 365-76 (2011).
9. Arvanitakis Z, Wilson RS, Bienias JL, Evans DA, Bennett DA. Diabetes mellitus and risk of Alzheimer disease and decline in cognitive function. *Arch Neurol*. **61**(5):661-6. (2014).
10. Arvanitakis Z, Schneider JA, Wilson RS, Li Y, Arnold SE, Wang Z, Bennett DA. Diabetes is related to cerebral infarction but not to AD pathology in older persons. *Neurology*. **12**;67(11):1960-5. (2006).
11. Talbot K1, Wang HY, Kazi H, Han LY, Bakshi KP, Stucky A, Fuino RL, Kawaguchi KR, Samoyedny AJ, Wilson RS, Arvanitakis Z, Schneider JA, Wolf BA, Bennett DA, Trojanowski JQ, Arnold SE. Demonstrated brain insulin resistance in Alzheimer's disease patients is associated with IGF-1 resistance, IRS-1 dysregulation, and cognitive decline. *J Clin Invest*. **122**(4):1316-38. (2012).
12. Hohman TJ, Chibnik L, Bush WS, Jefferson AL, De Jaeger PL, Thornton-Wells TA, Bennett DA, Schneider JA. GSK3 β Interactions with Amyloid Genes: An Autopsy Verification and Extension. *Neurotox Res*. **28**(3):232-8. (2015).
13. Karki, R., Kodamullil, A. T., Hofmann-Apitius, M. Comorbidity Analysis between Alzheimer's Disease and Type 2 Diabetes Mellitus (T2DM) Based on Shared Pathways and the Role of T2DM Drugs. *J Alzheimers Dis*. **60**, 721-731 (2017).
14. Bennett DA, Schneider JA, Arvanitakis Z, Wilson RS. Overview and findings from the religious orders study. *Curr Alzheimer Res*. 2012a; **9**(6):628.

15. Bennett DA, Schneider JA, Buchman AS, Barnes LL, Boyle PA, Wilson RS. Overview and findings from the Rush Memory and Aging Project. *Curr Alzheimer Res.* 2012b; 9(6):646.
16. Huan, T., Meng, Q., Saleh, M. A., Norlander, A. E., Joehanes, R., Zhu, J., Chen, B. H., Zhang, B., Johnson, A. D., Ying, S., Courchesne, P., Raghavachari, N., Wang, R., Liu, P., O'Donnell, C. J., Vasani, R., Munson, P. J., Madhur, M. S., Harrison, D. G., Yang, X., Levy, D. Integrative network analysis reveals molecular mechanisms of blood pressure regulation. *Mol Syst Biol.* **11**, 799 (2015).
17. Jiang, P., Scarpa, J. R., Fitzpatrick, K., Losic, B., Gao, V.D., Hao, K., Summa, K.C., Yang, H. S., Zhang, B., Allada, R., Vitaterna, M. H., Turek, F. W., Kasarskis, A. A systems approach identifies networks and genes linking sleep and stress: implications for neuropsychiatric disorders. *Cell Rep.* **11**, 835-848 (2015)
18. Schwartz, S. M., Schwartz, H. T., Horvath, S., Schadt, E., Lee, S. I. (2012). A systematic approach to multifactorial cardiovascular disease: causal analysis. *Arterioscler Thromb Vasc Biol.* **32**, 2821-2835 (2012).
19. Peters J, Janzing D, Schölkopf B. (2011). Causal inference on discrete data using additive noise models. *IEEE Trans Pattern Anal Mach Intell.* 33(12):2436-2450.
20. Peters, J., Janzing, D., and Schölkopf, B. Elements of Causal Inference: Foundations and Learning Algorithms. *The MIT Press*, Boston (2017).
21. Pearl, J. Causality. New York: *Cambridge University Press*, (2000).
22. Cussens, J. Integer Programming for Bayesian Network Structure Learning. *Quality Technology & Quantitative Management.* **11**, 99-110 (2014).
23. Devasia, J. V. & Chandran, P. Inferring disease causing genes and their pathways: A mathematical perspective. arXiv:1611.02538. (2016).
24. Quek, L. E. & Nielsen, L. K. A depth-first search algorithm to compute elementary flux modes by linear programming. *BMC Syst Biol.* **8**, 94 (2014).
25. Jindalertudomdee, J., Hayashida, M. & Akutsu T. Enumeration Method for Structural Isomers Containing User-Defined Structures Based on Breadth-First Search Approach. *J Comput Biol.* **23**, 625-640 (2016).
26. Tang, X., Wang, J., Li, M., He, Y. & Pan, Y. A novel algorithm for detecting protein complexes with the breadth first search. *Biomed Res Int.* **Article ID** , 354539 (2014).
27. Peters, J., Janzing, D., Schölkopf, B. (2011). Causal Inference on Discrete Data using Additive Noise Models. *IEEE Transactions on Pattern Analysis and Machine Intelligence (TPAMI)* . **33**, 2436-2450.
28. Janzing, D., and Steudel, B. (2010). Justifying additive-noise-model based causal discovery via algorithmic information theory. *Open Systems and Information Dynamics.* 17, 189–212.
29. Peters, J., Janzing, D., Schölkopf, B. (2017). Elements of Causal Inference - Foundations and Learning Algorithms Adaptive Computation and Machine Learning Series, The MIT Press, Cambridge, MA, USA.
30. Xiong, M. M. Big data in omics and imaging: integrated analysis and causal inference. CRC Press. (2018).

31. Parascandolo, G., Kilbertus, N., Rojas-Carulla, M., Schölkopf, B. Learning Independent Causal Mechanisms. Proceedings of the 35th International Conference on Machine Learning (ICML), 80, pages: 4033-4041, Proceedings of Machine Learning Research, (Editors: Dy, Jennifer and Krause, Andreas), PMLR, 2018 (conference)
32. Kandel, E. R. The molecular biology of memory: cAMP, PKA, CRE, CREB-1, CREB-2, and CPEB. *Kandel Molecular Brain*. **5**, 14. (2012).
33. Saura, C. A. & Valero, J. The role of CREB signaling in Alzheimer's disease and other cognitive disorders. *Rev Neurosci*. **22**, 153-69 (2011).
34. White, C. C. *et al.* Identification of genes associated with dissociation of cognitive performance and neuropathological burden: Multistep analysis of genetic, epigenetic, and transcriptional data. *PLoS Med*. **14**, e1002287 (2017).
35. Cerasuolo, J. & Izzo, A. Persistent impairment in working memory following severe hyperglycemia in newly diagnosed type 2 diabetes. *Endocrinol Diabetes Metab Case Rep*. 2017 Dec 12;2017. pii: 17-0101. doi: 10.1530/EDM-17-0101. eCollection 2017.
36. Huang, R. R. *et al.* Spatial working memory impairment in primary onset middle-age type 2 diabetes mellitus: An ethology and BOLD-fMRI study. *J Magn Reson Imaging*. 75-87 (2016).
37. Montoya JC, Fajardo D, Peña A, Sánchez A, Domínguez MC, Satizábal JM, García-Vallejo F. Global differential expression of genes located in the Down Syndrome Critical Region in normal human brain. *Colomb Med (Cali)*. 45(4):154-161 (2014).
38. Kohli MA, Cukier HN, Hamilton-Nelson KL, Rolati S, Kunkle BW, Whitehead PL, Züchner SL, Farrer LA, Martin ER, Beecham GW, Haines JL, Vance JM, Cuccaro ML, Gilbert JR, Schellenberg GD, Carney RM, Pericak-Vance MA. Segregation of a rare TTC3 variant in an extended family with late-onset Alzheimer disease. *Neurol Genet*. 2(1):e41 (2016).
39. Berto G, Camera P, Fusco C, Imarisio S, Ambrogio C, Chiarle R, Silengo L, Di Cunto F. The Down syndrome critical region protein TTC3 inhibits neuronal differentiation via RhoA and Citron kinase. *J Cell Sci*. 120(Pt 11):1859-1867 (2007).
40. aria II, Fegley AJ, Nicholl SM, Roztocil E, Davies MG. Differential regulation of ERK1/2 and p38(MAPK) by components of the Rho signaling pathway during sphingosine-1-phosphate-induced smooth muscle cell migration. *J Surg Res*. 122(2):173-179 (2004).
41. Maiese K. Forkhead Transcription Factors: Formulating a FOXO Target for Cognitive Loss. *Curr Neurovasc Res*. 14(4):415-420 (2017).
42. Kim JH, Choi JS, Lee BH. PI3K/Akt and MAPK pathways evoke activation of FoxO transcription factor to undergo neuronal apoptosis in brain of the silkworm *Bombyx mori* (Lepidoptera: Bombycidae). *Cell Mol Biol (Noisy-le-grand)*. Suppl.58:OL1780-1785 (2012).
43. Zhang Z, Amorosa LF, Coyle SM, Macor MA, Birnbaum MJ, Lee LY, Haimovich B. Insulin-Dependent Regulation of mTORC2-Akt-FoxO Suppresses TLR4 Signaling in

- Human Leukocytes: Relevance to Type 2 Diabetes. *Diabetes Res Clin Pract.* 128:127-135 (2017).
44. Yin X, Xu Z, Zhang Z, Li L, Pan Q, Zheng F, Li H. Association of PI3K/AKT/mTOR pathway genetic variants with type 2 diabetes mellitus in Chinese. *Diabetes Res Clin Pract.* 128:127-135 (2017).
 45. Kitagishi Y, Nakanishi A, Minami A, Asai Y, Yasui M, Iwaizako A, Suzuki M, Ono Y, Ogura Y, Matsuda S. Certain Diet and Lifestyle May Contribute to Islet β -cells Protection in Type-2 Diabetes via the Modulation of Cellular PI3K/AKT Pathway. *Open Biochem J.* 8:74-82 (2014).
 46. Mohammad Ahmadi Soleimani S, Ekhtiari H, Cadet JL. Drug-induced neurotoxicity in addiction medicine: From prevention to harm reduction. *Prog Brain Res.* 223:19-41 (2016).
 47. Yang SP, Muo CH, Wang IK, Chang YJ, Lai SW, Lee CW, Morisky DE. Risk of type 2 diabetes mellitus in female breast cancer patients treated with morphine: A retrospective population-based time-dependent cohort study. *Diabetes Res Clin Pract.* 110(3):285-290 (2015).
 48. Gohlke JM, Thomas R, Zhang Y, Rosenstein MC, Davis AP, Murphy C, Becker KG, Mattingly CJ, Portier CJ. Genetic and environmental pathways to complex diseases. *BMC Syst Biol.* 2009 May 5;3:46 (2009).
 49. de Jager CA, Kovatcheva A. Summary and discussion: Methodologies to assess long-term effects of nutrition on brain function. *Nutr Rev.* 68 Suppl 1:S53-8 (2010).
 50. Hooper C, De Souto Barreto P, Pahor M, Weiner M, Vellas B. The Relationship of Omega 3 Polyunsaturated Fatty Acids in Red Blood Cell Membranes with Cognitive Function and Brain Structure: A Review Focussed on Alzheimer's Disease. *J Prev Alzheimers Dis.* 5(1):78-84 (2018).
 51. Grimm MOW, Michaelson DM, Hartmann T. Omega-3 fatty acids, lipids, and apoE lipidation in Alzheimer's disease: a rationale for multi-nutrient dementia prevention. *J Lipid Res.* 58(11):2083-2101 (2017).
 52. Ramalho RM, Viana RJ, Low WC, Steer CJ, Rodrigues CM. Bile acids and apoptosis modulation: an emerging role in experimental Alzheimer's disease. *Trends Mol Med.* 14(2):54-62 (2008).
 53. Pan X, Elliott CT, McGuinness B, Passmore P, Kehoe PG, Hölscher C, McClean PL, Graham SF, Green BD. Metabolomic Profiling of Bile Acids in Clinical and Experimental Samples of Alzheimer's Disease. *Metabolites.* 7(2). pii: E28 (2017).
 54. Bouchouirab FZ, Fortin M, Noll C, Dubé J, Carpentier AC. Plasma Palmitoyl-Carnitine (AC16:0) is a Marker of Increased Postprandial Nonesterified Incomplete Fatty Acid Oxidation Rate in Individuals with Type 2 Diabetes. *Can J Diabetes.* 2017 Nov 9. pii: S1499-2671(17)30177-6.
 55. Wang S, Deng Y, Xie X, Ma J, Xu M, Zhao X, Gu W, Hong J, Wang W, Xu G, Ning G, Gu Y, Zhang Y. Plasma bile acid changes in type 2 diabetes correlated with insulin secretion in

- two-step hyperglycemic clamp. *J Diabetes*. 2018 Apr 17. doi: 10.1111/1753-0407.12771. [Epub ahead of print].
56. Chávez-Talavera O, Tailleux A, Lefebvre P, Staels B. Bile Acid Control of Metabolism and Inflammation in Obesity, Type 2 Diabetes, Dyslipidemia, and Nonalcoholic Fatty Liver Disease. *Gastroenterology*. 152(7):1679-1694.e3 (2017).
 57. Grimm MO, Mett J, Grimm HS, Hartmann T. APP Function and Lipids: A Bidirectional Link. *Front Mol Neurosci*. 10:63 (2017).
 58. Huang YT, Iwamoto K, Kurosaki T, Nasu M, Ueda S. The neuronal POU transcription factor Brn-2 interacts with Jab1, a gene involved in the onset of neurodegenerative diseases. *Neurosci Lett*. 382(1-2):175-8 (2005).
 59. Martorana A, Koch G. "Is dopamine involved in Alzheimer's disease?". *Front Aging Neurosci*. 6:252 (2014).
 60. Nobili A, Latagliata EC, Viscomi MT, Cavallucci V, Cutuli D, Giacobuzzo G, Krashia P, Rizzo FR, Marino R, Federici M, De Bartolo P, Aversa D, Dell'Acqua MC, Cordella A, Sancandi M, Keller F, Petrosini L, Puglisi-Allegra S, Mercuri NB, Coccorello R, Berretta N, D'Amelio M. Dopamine neuronal loss contributes to memory and reward dysfunction in a model of Alzheimer's disease. *Nat Commun*. 8:14727 (2017).
 61. Yokoyama AS, Rutledge JC, Medici V. DNA methylation alterations in Alzheimer's disease. *Environ Epigenet*. 3(2):dvx008 (2017).
 62. Nagata K, Mano T, Murayama S, Saido TC, Iwata A. DNA methylation level of the neprilysin promoter in Alzheimer's disease brains. *Neurosci Lett*. 670:8-13 (2018).
 63. Shen J, Zhu B. Integrated analysis of the gene expression profile and DNA methylation profile of obese patients with type 2 diabetes. *Mol Med Rep*. 17(6):7636-7644 (2018).

 64. Elliott HR, Shihab HA, Lockett GA, Holloway JW, McRae AF, Smith GD, Ring SM, Gaunt TR, Relton CL. Role of DNA Methylation in Type 2 Diabetes Etiology: Using Genotype as a Causal Anchor. *Diabetes*. 66(6):1713-1722 (2017).
 65. Domise M, Vingtdoux V. AMPK in Neurodegenerative Diseases. *EXS*. 107:153-177 (2016).
 66. Coughlan KA, Valentine RJ, Ruderman NB, Saha AK. AMPK activation: a therapeutic target for type 2 diabetes? *Diabetes Metab Syndr Obes*. 7:241-53 (2014).
 67. Boyd S, Parikh N, Chu E, Peleato B, and Eckstein J. (2011). Distributed optimization and statistical learning via the alternating direction method of multipliers. *Foundations and Trends in Machine Learning*, 3(1):1–122.
 68. Parikh N and Boyd S. (2014). Proximal Algorithms. *Foundations and Trends in Optimization*, 1(3):123-231.
 69. Udell M, Horn C, Zadeh R, Boyd S. (2016). Generalized Low Rank Models. *Foundations and Trends® in Machine Learning*. 9(1):1-118.

Acknowledgements

Mr. Hu and Mr. Jin were supported by National Natural Science Foundation of China (31521003), Shanghai Municipal Science and Technology Major Project (2017SHZDZX01), and the 111 Project (B13016) from Ministry of Education.

Author contributions

Z.H, R. J, P. W, Y.Z developed software and conducted data analysis, M.X designed project and wrote manuscript, L. J, J. Z and J. W designed the project, D. B provided data and wrote manuscript, P. J provided data.

Additional information

Complete financial interests. The authors declare no competing financial interests.

Figure

Figure 1. Scheme of multilevel omic networks.

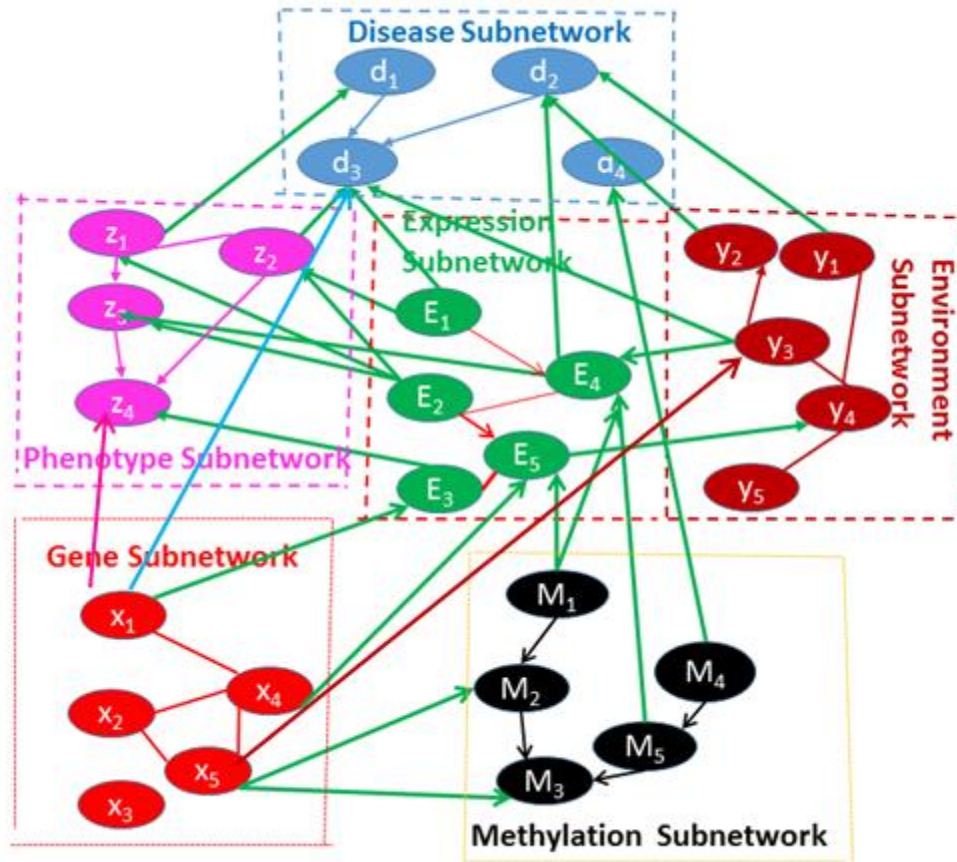


Figure 2. (A) Shared CREBBP, MAPK and PI3K-AKT pathways between AD and T2DM; (B) Shared causal subnetwork structure from CREBBP to AD and T2DM.

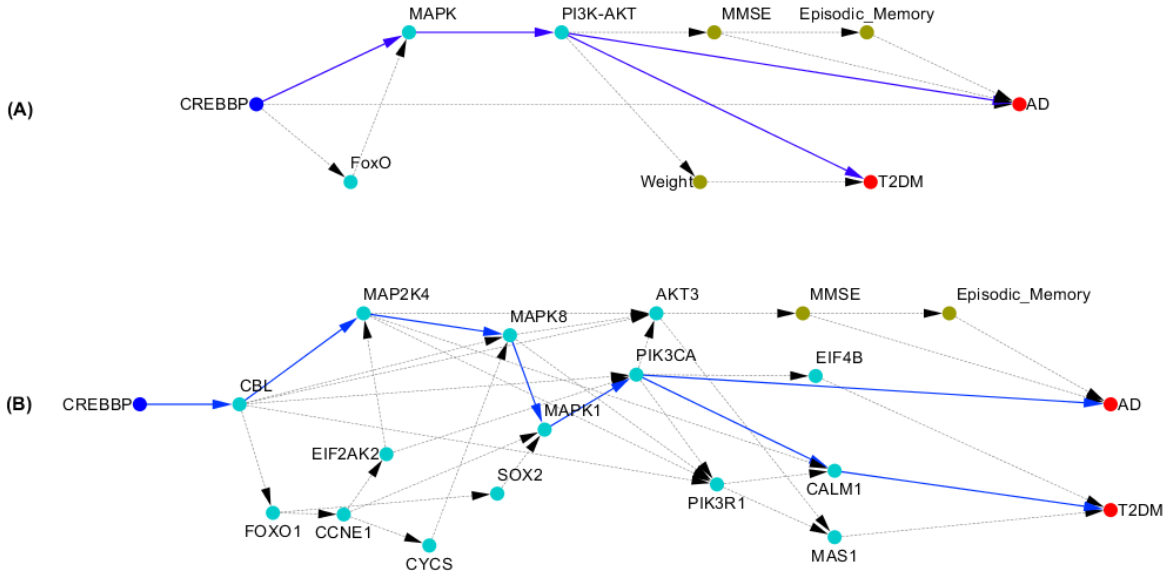


Figure 3. (A) Shared TTC3, FoxO, MAPK, and PI3K-AKT Pathways between AD and T2DM; (B) Shared causal subnetwork structure from TTC3 to AD and T2DM.

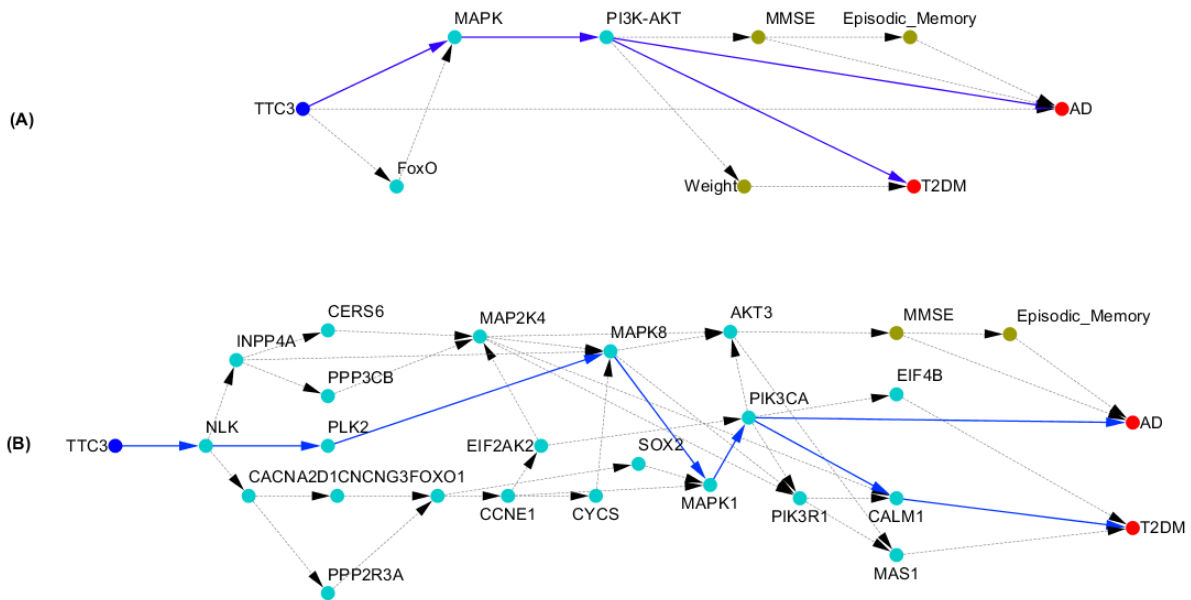


Figure 4. (A) Shared APP, Fatty Acid Biosynthesis and Primary Bile Acid Biosynthesis Pathways between AD and T2DM; (B) Shared causal subnetwork structure from APP to AD and T2DM.

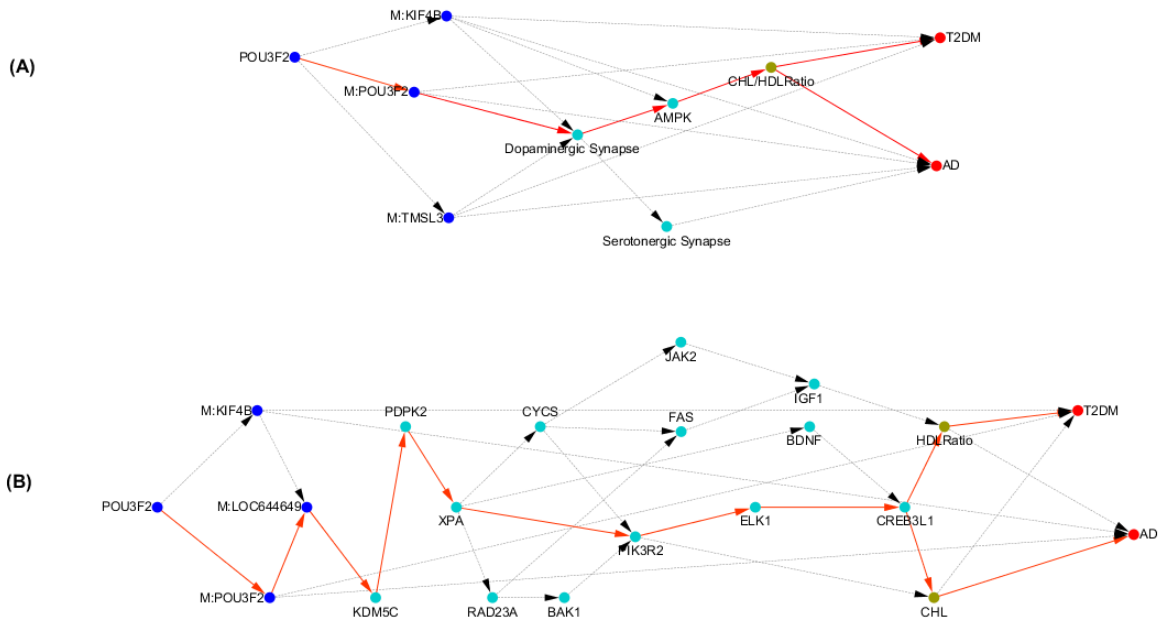
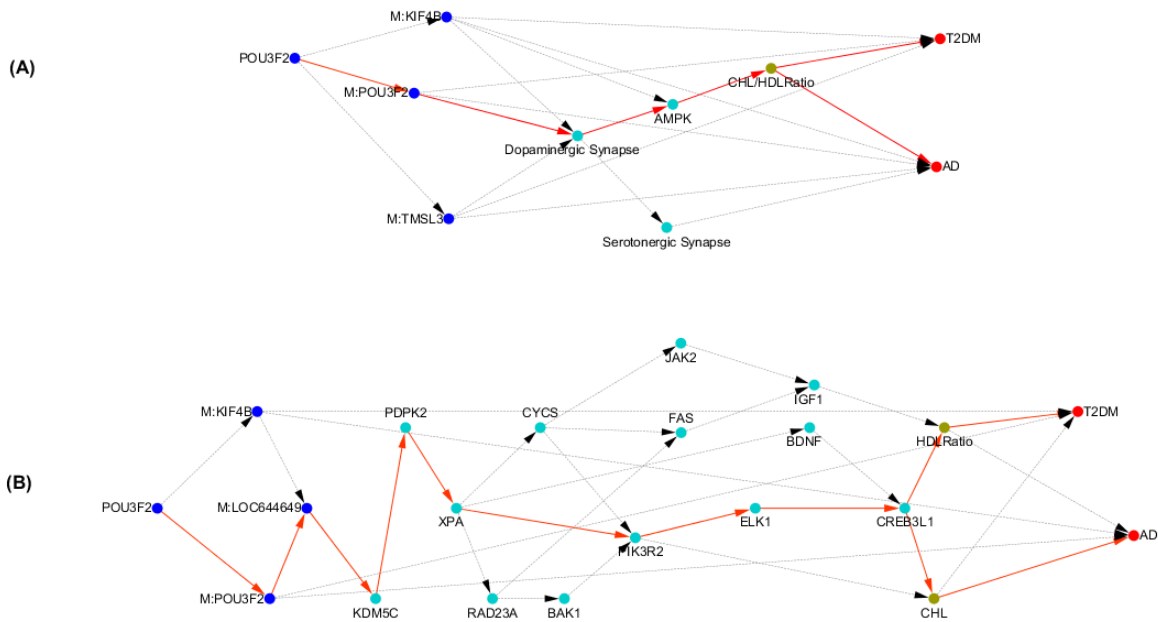


Figure 5. (A) Shared Methylated Genes POU3F2, KIF4B and TNSL3, and Dopaminergic Synapse and AMPK Pathways between AD and T2DM; (B) Shared causal subnetwork structure from POU3F2 to AD and T2DM.



Supplementary Figure

Figure S1. (A) Shared morphine addiction and neuroactive ligand receptor interaction pathways between AD and T2DM; (B) Shared causal subnetwork structure from HNF4G to AD and T2DM.

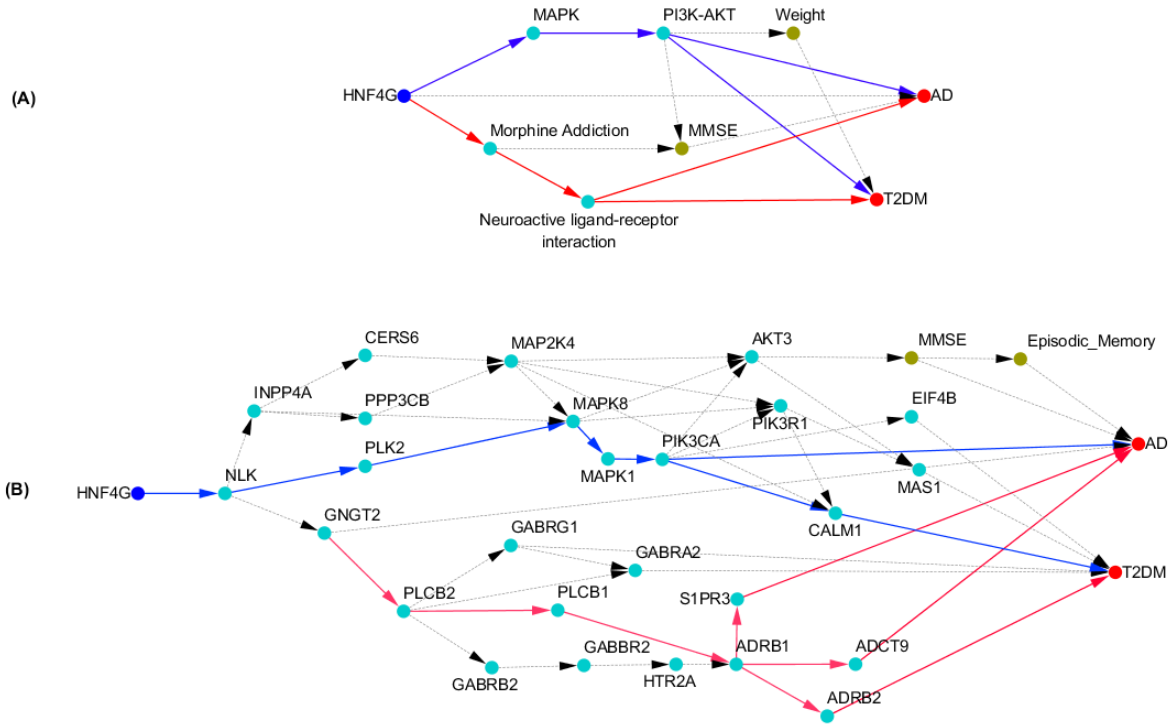


Figure S2. Average expression levels of genes in Figure 4 for AD, T2DM and normal individuals where gene expression levels were normalized.

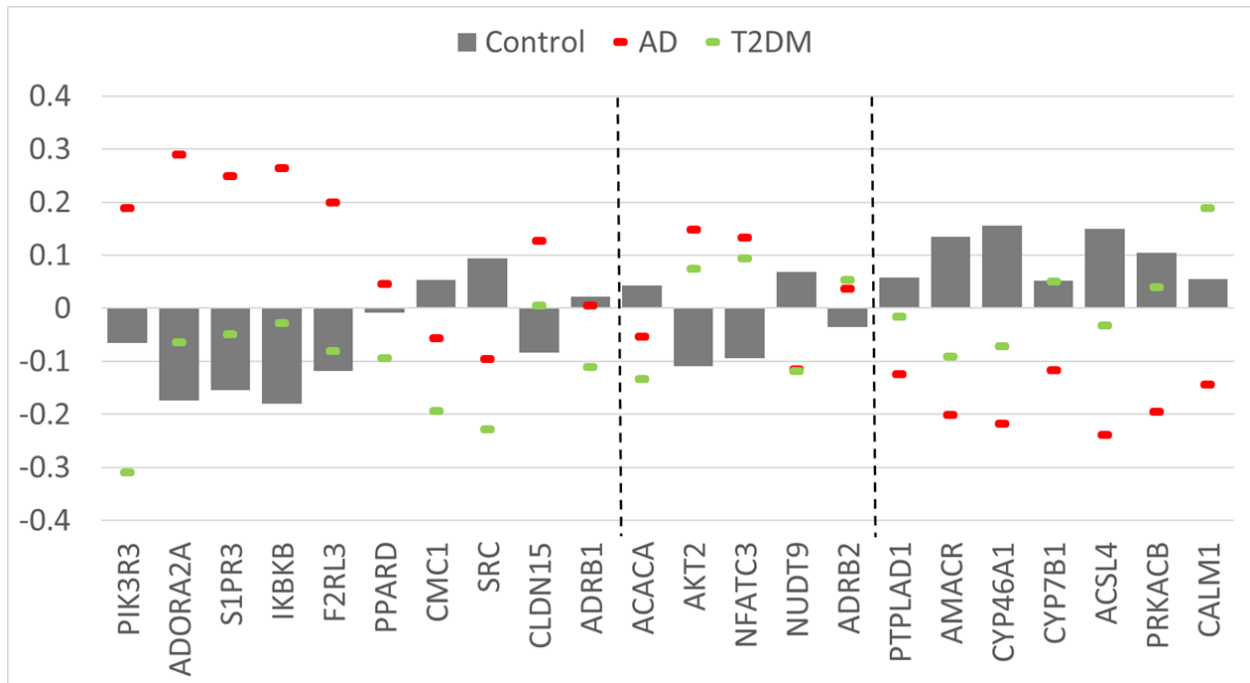
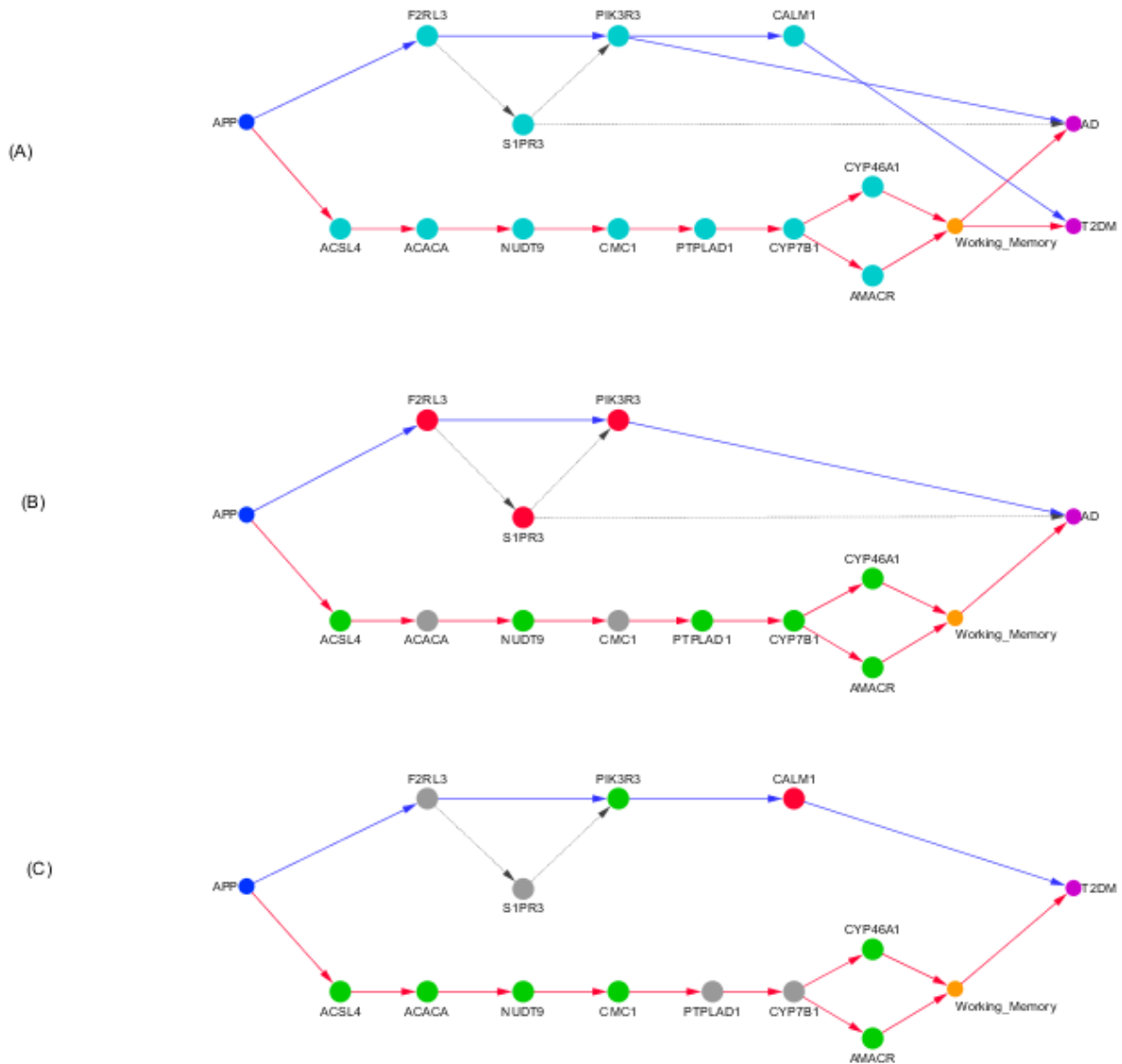


Figure S3. (A) Two major causal paths from APP to AD and T2DM in Figure 4; (B) Differential expressions of the genes along two major causal paths in (A) between AD and normal individuals where the nodes in red color represented over expressed genes, the nodes in green color represented the under expressed genes and the nodes in the grey color represented the genes showing no differential expressions; (C) Differential expressions of the genes along two major causal paths in (A) between T2DM and normal individuals where the nodes in red color represented over expressed genes, the nodes in green color represented the under expressed genes and the nodes in the grey color represented the genes showing no differential expressions.



Supplementary Table

Table S1

Gene	T2DM		AD	
	Causation	Association	Causation	Association
GTF2H2C	<E-06	0.000156	<E-06	0.075045
NAIP	<E-06	0.000785	<E-06	0.057792
RN7SL9P	<E-06	0.000156	<E-06	0.075045
RP11-497H16.5	<E-06	0.001671	<E-06	0.182268
RP11-497H16.6	<E-06	0.000334	<E-06	0.200074
SERF1B	<E-06	0.000447	<E-06	0.163819
SMN2	<E-06	0.000447	<E-06	0.163819
ZNF658B	<E-06	0.867831	<E-06	0.102522

Table S2

	AD		T2DM	
	Causation	Association	Causation	Association
LINC01123	<E-06	0.209055802	<E-06	0.007821734
ZBTB45P1	<E-06	0.209055802	<E-06	0.007821734
GTF2H2C	<E-06	0.045337348	<E-06	0.000155933
NAIP	<E-06	0.023560082	<E-06	0.000785176
RN7SL9P	<E-06	0.075045141	<E-06	0.000155933
RP11-497H16.5	<E-06	0.027245868	<E-06	0.001670784
RP11-497H16.6	<E-06	0.106195835	<E-06	0.000334017
SERF1B	<E-06	0.017756029	<E-06	0.000446698
SMN2	<E-06	0.017756029	<E-06	0.000446698
RN7SL763P	<E-06	0.242608501	<E-06	0.887587122
RANP9	<E-06	0.153098533	<E-06	0.206418787
ZNF658B	<E-06	0.006744952	<E-06	0.203671552
AC132872.2	<E-06	0.118907963	<E-06	0.047484691

Table S3

	AD		T2DM	
	Causation	Association	Causation	Association
IGKV6D-21	<E-06	0.00936		0.00838
RN7SL632P	<E-06	0.00053		0.10824
CDH18	<E-06	0.00736		0.11987
HLA-DRB5	<E-06	0.01958		0.01317
RPL3P2	<E-06	0.00391		0.05737
FAM74A6	<E-06	0.00256		0.17522
RNU6-156P	<E-06	0.00209		0.00086
RP11-15J10.1	<E-06	0.00876		0.01246
RP11-262H14.4	<E-06	0.00173		0.01412
RP11-318K12.2	<E-06	0.0031		0.00086
RNU6-702P	<E-06	0.01116		0.26546
AL021920.1	<E-06	0.00529		0.10803
AL590452.1	<E-06	0.0034		0.01512
EIF1AXP1	<E-06	0.00529		0.10803
FAM231B	<E-06	0.00187		0.28261
PRAMEF11	<E-06	0.00122		0.07388
RP5-845O24.8	<E-06	0.00122		0.07388
TTC3	<E-06	0.0102		0.01343
AC009237.16	<E-06	0.0024		0.17164
AC009237.17	<E-06	0.0024		0.17164

Table S4

Gene	P-value			
	Causation		Association	
	AD	T2DM	AD	T2DM
PLA2G15	<0.0001	0.6633	0.0012	0.7645
GRPEL2	<0.0001	0.3611	0.0026	0.9894
TCEAL6	<0.0001	0.7324	0.0001	0.3729
C19orf71	<0.0001	0.8063	0.0002	0.4285
GRTP1	<0.0001	0.7326	0.0004	0.4044
CTC-471C19.1	<0.0001	0.9039	<0.0001	0.8677
GAP43	<0.0001	0.413	0.0001	0.2183
NTNG1	<0.0001	0.2216	<0.0001	0.298
BIN1	<0.0001	0.9583	0.4087	0.809
ZNF683	<0.0001	0.5699	0.0098	0.391
PIGS	<0.0001	0.361	0.0624	0.7423
MRPS18A	<0.0001	0.4478	0.0004	0.8081
PRKCD	0.0001	0.5847	0.0006	0.0814
FNDC5	0.0001	0.8283	0.0000	0.9253
SLC7A14	0.0001	0.9696	0.0101	0.7183
GRAMD1B	0.0001	0.0005	0.0171	0.6413
USP12	0.0001	0.5937	0.041	0.0269
DHRS7	0.0001	0.9111	0.0571	0.4734
OAZ1	0.0001	0.7556	0.0089	0.6632

Table S5

Gene	P-value			
	Causation		Association	
	T2DM	AD	T2DM	AD
GRN	<0.0001	0.3019	<0.0001	0.3037
ATP1B3	<0.0001	0.3848	<0.0001	0.3358
CTD-3065J16.6	<0.0001	0.5351	0.4403	0.2133
BX571672.1	<0.0001	0.587	0.5182	0.3088
SLC25A35	<0.0001	0.7881	0.6975	0.3619
PRR12	<0.0001	0.9786	0.3704	0.281
AOC3	<0.0001	0.9936	0.1873	0.0678

Table S6

Methylated Gene	P-value	
	Causation	Association
EMX2OS	< 1e-4	0.1973
PIPOX	< 1e-4	0.6245
DHX8	< 1e-4	0.7317
cg04413644	< 1e-4	0.0086
cg12049093	< 1e-4	0.1122
cg21346589	< 1e-4	0.235
cg18527583	< 1e-4	0.0126
cg00639635	< 1e-4	0.2032
cg22133973	< 1e-4	0.0004
cg12644659	< 1e-4	0.7813
cg12949927	< 1e-4	0.0915
cg20714487	< 1e-4	0.0000
cg03701930	< 1e-4	0.5572
CARKD	< 1e-4	0.2309
NYNRIN	< 1e-4	0.1213
IL2RA	< 1e-4	0.8899
cg02438164	< 1e-4	0.0029

Table S7

Methylated Gene	P-value	
	Causation	Association
cg27424148	< 1e-4	0.8752
MIR220B	< 1e-4	0.3568
cg16991316	< 1e-4	0.0292
cg01433468	< 1e-4	0.4165
cg04124260	< 1e-4	0.0587
cg06769739	< 1e-4	0.0004
cg11989330	< 1e-4	0.0006
cg17883371	< 1e-4	0.0075
GSTTP1	< 1e-4	0.0016
YWHAQ	< 1e-4	0.6393
cg25004193	< 1e-4	0.0001
cg25757820	< 1e-4	0.2169
cg02093808	< 1e-4	0.2378
C11orf45	< 1e-4	0.1566
cg00850073	< 1e-4	0.0136
NME5	< 1e-4	0.1576
cg14727987	< 1e-4	0.0011
cg10245123	< 1e-4	0.0014
MFHAS1	< 1e-4	0.5626
cg11388673	< 1e-4	0.6857
cg18001780	< 1e-4	0.0127
KRT77	< 1e-4	0.0291
cg16624888	< 1e-4	0.0000
TPT1	< 1e-4	0.2871
CCDC70	< 1e-4	0.0186
cg01358406	< 1e-4	0.0119
cg03608502	< 1e-4	0.1001

Table S8. A list of 120 DNA methylation sites/genes that were indirectly connected to AD and T2DM.

Methylation Site/Gene	Expressed Genes	P-value		Reference Methylation Site in the Gene
		Causation	Association	
cg18747197	QKI	0.00004	4.04E-06	
cg19351026	GABRA2	0.00018	1.01E-05	
cg27665808	snoU13	0.00014	1.17E-05	
GSTTP1	RP11-259G18.2	0.00007	1.55E-05	cg10678937, cg11141652, cg15242686, cg22666875
cg12363375	CTD-3025N20.2	0.00021	1.98E-05	
cg16677162	GPX6	0.00011	2.24E-05	
cg13401079	RCOR1	0.00015	2.77E-05	
cg17670237	RP11-259G18.2	0.00015	2.77E-05	
cg07536144	U1	0.00001	4.58E-05	
ABCA10	RP11-86H7.7	0.0001	4.64E-05	cg13849142, cg14019757, cg14069205
cg22463795	GABRA2	0.00019	4.65E-05	
cg01797450	ASS1	8.00E-05	5.03E-05	
cg23454003	PSMB6	9.00E-05	5.45E-05	
cg05455747	ZC3H4	0.00E+00	6.23E-05	
cg17526301	GPX6	3.00E-05	8.06E-05	
cg10061805	PPIAP2	1.80E-04	1.53E-04	
cg02190400	ZC3H4	5.00E-05	1.66E-04	
cg15304404	RXFP4	2.80E-04	1.83E-04	
cg24751928	CTD-2501E16.2	4.00E-05	1.96E-04	
cg17125990	GABRA2	3.00E-05	2.06E-04	

Methylation Site/Gene	Expressed Genes	P-value		Reference Methylation Site in the Gene
		Causation	Association	
cg00415011	GARNL3	0.00E+00	2.08E-04	
cg23340218	WNT3A	3.00E-05	2.45E-04	
cg26274929	UTP6	5.00E-05	2.66E-04	
cg09977969	CTD-2116F7.1	2.00E-04	2.68E-04	
cg02461269	CTD-3025N20.2	6.00E-05	3.15E-04	
cg02523270	GARNL3	3.60E-04	3.24E-04	
cg09550810	GARNL3	2.00E-05	3.80E-04	
cg07475973	RP11-265D19.6	1.20E-04	3.91E-04	
cg21686890	ABCB6	2.00E-05	3.98E-04	
cg21099148	snoU13	1.90E-04	4.26E-04	
cg01870681	GPX6	1.90E-04	4.40E-04	
cg25112877	WNT3A	1.40E-04	4.63E-04	
cg19711815	RP11-259G18.2	8.00E-05	5.49E-04	
cg06447341	TTC37	3.00E-05	6.86E-04	
ch.2.3048096R	ASS1	2.00E-05	7.17E-04	
cg07536144	PLCH1-AS1	9.00E-05	7.44E-04	
cg15426660	snoU13	1.00E-05	7.61E-04	
cg08209099	RP11-259G18.2	7.00E-05	7.85E-04	
cg22891595	GARNL3	1.00E-05	8.71E-04	
cg06181286	CBLN4	0.00E+00	9.85E-04	
cg14739859	RP11-259G18.2	5.00E-05	9.89E-04	
cg12548341	GNAL	1.30E-04	1.06E-03	

Methylation Site/Gene	Expressed Genes	P-value		Reference Methylation Site in the Gene
		Causation	Association	
cg15426660	SNTB2	9.00E-05	1.16E-03	
cg10059756	GABRA2	4.00E-05	1.21E-03	
cg21205865	snoU13	4.00E-05	1.32E-03	
cg00039801	RP11-259G18.2	6.00E-05	1.35E-03	
cg10316834	snoU13	1.00E-04	1.35E-03	
cg20078879	RPS4X	9.00E-05	1.37E-03	
cg24015081	CTD-2176I21.1	1.80E-04	1.45E-03	
cg25214310	SUGT1	3.70E-04	1.53E-03	
cg14687029	ABCB6	8.00E-05	1.56E-03	
cg05157340	RANBP2	1.40E-04	2.00E-03	
cg06709828	CTD-3025N20.2	0.00E+00	2.08E-03	
cg06112654	SNTB2	4.00E-05	2.09E-03	
cg06112654	snoU13	6.00E-05	2.18E-03	
cg22651787	FAM188B	5.00E-05	2.50E-03	
cg14577406	RBPM2	0.00E+00	2.58E-03	
cg04854637	SUGT1	3.00E-05	3.27E-03	
cg12180270	GABRA2	2.00E-05	3.31E-03	
cg04606076	RXFP4	1.20E-04	3.32E-03	
cg02486332	CASP12	1.20E-04	3.43E-03	
cg11868247	RP11-351K16.4	7.00E-05	3.50E-03	
cg13001963	RXFP4	0.00E+00	3.99E-03	
cg24430419	snoU13	1.00E-04	4.03E-03	

Methylation Site/Gene	Expressed Genes	P-value		Reference Methylation Site in the Gene
		Causation	Association	
cg07716131	SAA1	1.60E-04	4.57E-03	
MIR145	RCOR1	3.00E-05	4.80E-03	cg01310120, cg08537847, cg11671363, cg22941668, cg23917868, cg27083040
cg16101962	GARNL3	2.00E-05	4.95E-03	
cg10238080	snoU13	6.30E-04	5.01E-03	
cg12094552	SNTB2	5.00E-05	5.25E-03	
cg23346544	ARHGAP20	0.00E+00	5.56E-03	
cg13332807	PKN2	1.30E-04	6.11E-03	
TDGF1	ST6GALNAC6	5.00E-05	7.25E-03	cg06174858
cg24617444	RUSC1	0.00E+00	7.76E-03	
ANKRD53	CPE	2.10E-04	7.92E-03	cg00421335, cg01154254, cg04076766, cg04737087, cg05472974, cg05492660, cg06783668, cg07903989, cg12428298, cg15165122, cg18006568, cg18313051, cg19111030, cg19244342, cg19490001, cg20814026, cg22050950, cg23060872, cg24573743, cg27665449
cg20918393	PPIAP2	9.00E-05	8.20E-03	
cg23925513	RARB	1.20E-04	8.65E-03	
cg18105749	BRSK2	5.00E-05	9.15E-03	
cg16624888	RXFP4	6.00E-05	9.48E-03	
cg09315586	SUGT1	1.00E-05	9.81E-03	
cg20078879	DNAJC1	7.00E-05	1.01E-02	

Methylation Site/Gene	Expressed Genes	P-value		Reference Methylation Site in the Gene
		Causation	Association	
cg00651087	ZNF114	5.00E-05	1.12E-02	
cg04606076	C2CD2L	1.50E-04	1.22E-02	
cg10061805	FAN1	1.90E-04	1.25E-02	
cg25900943	SNTB2	1.00E-05	1.31E-02	
HRCT1	DCTN2	2.80E-04	1.31E-02	cg02258201, cg05470166
cg05521150	PMS2CL	5.00E-05	1.44E-02	
cg11868247	CSNK1G1	7.00E-05	1.46E-02	
cg11868247	EIF6	6.00E-05	1.66E-02	
cg24631482	LA16c-444G7.2	0.00005	1.77E-02	
cg04858776	OR2L13	0.00015	1.86E-02	
cg15022039	SRD5A1	0.00033	1.90E-02	
C6orf223	SMO	0.00003	2.01E-02	cg02213045, cg04386144, cg09745336, cg10938046, cg11201894, cg13900100, cg15629096, cg16039071, cg18949415, cg19274606, cg24630373, cg25360181
cg17624891	DGKK	0.00007	2.04E-02	
cg25816127	WNT3A	0	2.08E-02	
cg26686150	FAM213B	0.00001	2.14E-02	
cg19937979	hsa-mir-146a	0.00002	2.15E-02	
cg04819760	FAH	0.00057	2.28E-02	
cg07929768	POTEG	1.60E-04	2.33E-02	
cg26095395	ADRA1B	0.00E+00	2.54E-02	

Methylation Site/Gene	Expressed Genes	P-value		Reference Methylation Site in the Gene
		Causation	Association	
cg14145524	XRCC5	0.00E+00	2.56E-02	
cg17214023	INPP5F	8.00E-05	2.59E-02	
cg16609139	SDS	1.30E-04	2.74E-02	
ch.11.96774805R	RPS4X	3.00E-05	2.79E-02	
ch.10.109266902R	RP11-351K16.4	0.00013	2.95E-02	
cg02796279	OR7C1	0.00004	3.29E-02	
cg19937979	NDUFA8	0.00003	3.42E-02	
ch.2.1894803R	NUMB	0.00006	3.44E-02	
cg14257429	SNTB2	0.00002	3.66E-02	
cg08122831	RP11-284N8.3	0.00001	3.78E-02	
cg11465213	EXOSC2	0.00006	4.05E-02	
cg05766107	ADCYAP1R1	0.00005	4.08E-02	
cg00895132	ZNF233	0.00003	4.19E-02	
cg19355069	ESD	0.00014	4.32E-02	
cg18978531	C2orf18	0.00009	4.72E-02	
MYCT1	RP11-265D19.6	0.00002	4.76E-02	cg02830467,cg15961007
cg03257930	FADS6	0.00003	4.81E-02	
cg11540476	RP11-114F3.5	0.00001	4.86E-02	